online commentary

Characterization of a novel binding partner of the melanocortin-4 receptor: attractin-like protein

Andrea M. HAQQ*[1,2], Patricia RENÉ*[1], Toshiro KISHI†, Kathy KHONG*, Charlotte E. LEE‡, Hongyan LIU§, Jeffrey M. FRIEDMAN§, Joel K. ELMQUIST†‡ and Roger D. CONE*[3]

*Vollum Institute, Oregon Health and Science University, Portland, OR 97239, U.S.A., †Department of Neurology, Beth Israel Deaconess Medical Center, and Program in Neuroscience, Harvard Medical School, Boston, MA 02215, U.S.A., ‡Department of Medicine and Division of Endocrinology, Beth Israel Deaconess Medical Center, Harvard Medical School, Boston, MA 02215, U.S.A., and §Rockefeller University, The Howard Hughes Medical Institute, New York, NY 10021, U.S.A.

The gene dosage effect of the MC4-R (melanocortin 4 receptor) on obesity suggests that regulation of MC4-R expression and function is critically important to the central control of energy homoeostasis. In order to identify putative MC4-R regulatory proteins, we performed a yeast two-hybrid screen of a mouse brain cDNA library using the mouse MC4-R intracellular tail (residues 303–332) as bait. We report here on one positive clone that shares 63 % amino acid identity with the C-terminal part of the mouse attractin gene product, a single-transmembrane-domain protein characterized as being required for agouti signalling through the melanocortin 1 receptor. We confirmed a direct interaction between this ALP (attractin-like protein) and the C-terminus of the mouse MC4-R by glutathione S-transferase pulldown experiments, and mapped the regions involved in this interaction using N- and C-terminal truncation constructs; residues 303–313 in MC4-R and residues 1280–1317 in ALP are required for binding. ALP is highly expressed in brain, but also in heart, lung, kidney and liver. Furthermore, co-localization analyses in mice showed co-expression of ALP in cells expressing MC4-R in a number of regions known to be important in the regulation of energy homoeostasis by melanocortins, such as the paraventricular nucleus of hypothalamus and the dorsal motor nucleus of the vagus.

Key words: attractin, glutathione S-transferase pull-down, G-protein-coupled receptor, melanocortin receptor, yeast two-hybrid.

INTRODUCTION

The pivotal role of the MC4-R (melanocortin 4 receptor) in the control of energy homoeostasis has been demonstrated both pharmacologically [1,2] and by several genetic models [3–5]. Blockade of the melanocortin signalling pathway leads to hyperphagia, reduced energy expenditure and, ultimately, obesity, as demonstrated by different genetic alterations, such as the ectopic expression of agouti in brain [6,7], overexpression of AGRP (agouti-related protein) [4,8], disruption of the POMC (pro-opiomelanocortin) gene precursor of α-melanocyte-stimulating hormone [5], and also by the deletion of MC4-R itself [3]. The relevance of these results has been confirmed conclusively by the discovery of mutations in the POMC and MC4-R genes that are responsible for an inherited obesity syndrome in humans [9–13]. Mutations in the MC4-R may be responsible for more than 3–4 % of severe early-onset obesity in children [14].

Moreover, the MC4-R seems to be tightly regulated, based on observations that mice heterozygous for the null MC4-R allele have an intermediate obese phenotype, and that haplo-insufficiency in humans can also cause obesity [15]. Thus regulation of energy homoeostasis through this pathway is highly susceptible to quantitative variations in MC4-R expression or function.

The MC4-R is expressed within every major subdivision of the CNS (central nervous system), including the cortex, thalamus, hypothalamus and brainstem [16,17]. To date, however, little is known about how this receptor finds its way to its site of action, how its signalling pathway is modulated, how the receptor is regulated by ligands, how it effects synaptic transmission, and what its full complement of physiological functions is. We have utilized the yeast two-hybrid assay in order to screen a mouse brain cDNA library for proteins that interact with the C-terminus of the MC4-R. One of these proteins is a novel mouse ALP (attractin-like protein). Mouse attractin is a single-transmembrane-domain protein encompassing 1428 amino acids that is encoded by the mouse *mahogany* locus. Loss of function in *mahogany* ($Atrn^{mg-3J}$/$Atrn^{mg-3J}$) mice blocks the ability of agouti protein in *lethal yellow* mice to antagonize the melanocortin 1 receptor in skin, and the central MC4-R [18–20]. However, the disruption of attractin is not able to suppress obesity in AGRP-overexpressing mice resulting from AGRP-induced MC4-R blockade [21]. Furthermore, attractin mRNA does not appear to exhibit a high degree of co-expression with the MC4-R [22], and thus attractin is unlikely to be involved in the regulation of MC4-R signalling by AGRP. We report here a new MC4-R-interacting partner, ALP, a protein which may regulate MC4-R function

Abbreviations used: AGRP, agouti-related protein; ALP, attractin-like protein; DEPC, diethyl pyrocarbonate; DMV, dorsal motor nucleus of the vagus; GFP, green fluorescent protein; G3PDH, glyceraldehyde-3-phosphate dehydrogenase; GST, glutathione S-transferase; IPTG, isopropyl β-D-thiogalactoside; ISHH, *in situ* hybridization histochemistry; MBP, maltose-binding protein; MC4-R, melanocortin 4 receptor; POMC, pro-opiomelanocortin; RT-PCR, reverse transcription–PCR.

[1] These authors contributed equally to this work.

[2] Present address: Department of Pediatrics, Duke University Medical Center, Division of Endocrinology and Diabetes, 306F A. Bell Building, Box 3080, Durham, NC 27710, U.S.A.

[3] To whom correspondence should be addressed (e-mail cone@ohsu.edu).

much as attractin regulates the function of the melanocortin 1 receptor.

EXPERIMENTAL

Yeast two-hybrid assay

Library screening

The *Saccharomyces cerevisiae* strains PJ69-2A (*MATa, trp1-901, leu2-3, 112, ura3-52, his3-200, gal4*Δ*, gal80*Δ*, LYS2::GAL1*$_{UAS}$*-GAL1*$_{TATA}$*-HIS3, GAL2*$_{UAS}$*-GAL2*$_{TATA}$*-ADE2*) and Y187 (*MAT*α*, ura3-52, his3-200, ade2-101, trp1-901, leu2-3, 112, gal4*Δ*, gal80*Δ*, met–, URA3::GAL1*$_{UAS}$*-GAL1*$_{TATA}$*-lacZ*) were used (Clontech, Palo Alto, CA, U.S.A.). Yeast strains were transformed with plasmid DNA using a small-scale LiAc Yeast Transformation Procedure (Yeast Protocols Handbook; Clontech). The yeast strains were grown in YPD medium (2 % peptone, 1 % yeast extract, 2 % glucose) before transformation. Transformants were selected on plates containing complete synthetic medium, which consisted of 0.17 % yeast nitrogen base (without amino acids and ammonium sulphate), 0.5 % ammonium sulphate, 2 % glucose, 2 % agar, adenine supplement and 3-AT (3-amino-1,2,4-triazole; a competitive inhibitor of yeast HIS3 protein). One or more amino acids were omitted from the medium depending on which plasmid was being selected.

The cDNA for the C-terminus of the MC4-R was cloned in-frame into the multiple cloning site of pGBKT7 (pGBKT7-MC4-R C-terminus) (Clontech). This construct was sequenced to verify the correct orientation and reading frame of the MC4-R C-terminus fused with the DNA-binding domain. This DNA-binding domain/MC4-R C-terminus protein was tested to ensure that there were no autonomous transcriptional activation or toxicity effects. A MATCHMAKER mouse brain cDNA library ($>1\times10^6$ independent clones) was cloned into a GAL4 activation domain vector, pACT2. This cDNA library was pretransformed in *S. cerevisiae* strain Y187. The bait, pGBKT7-MC4-R C-terminus (amino acids 303–332), was used to screen a pre-transformed mouse brain cDNA library using the supplied yeast mating procedure (Clontech). Colonies that grew successfully on the selective media (SD/ − Ade/ − His/ − Leu/ − Trp) were screened further for reporter gene β-galactosidase expression. The β-galactosidase assays were performed using replicas of colonies on filter paper. Colonies that were positive for β-galactosidase in less than 2 h were selected for further analysis. The positive colonies were restreaked several times on selective media and individual isolated colonies were rescreened for β-galactosidase activity, eliminating some false positives and ensuring that only one AD/library fusion plasmid was present in each Ade^+, His^+ or $LacZ^+$ colony. The target was also assayed for activation function in the presence of a bait vector without an insert, and the bait vector was assayed for activation function in the absence of the library vector, eliminating more false positives. Furthermore, a control bait vector containing lamin C was used to ensure that the library vector caused specific activation only in the presence of a bait vector containing the MC4-R C-terminus. To avoid analysing duplicate clones unnecessarily, they were characterized further by determining insert size using PCR amplification of the pACT2 inserts with vector-specific primers (Clontech). The PCR products were then digested with *Hae*III restriction enzyme and the restriction digestion patterns were compared. In order to determine the identity of unique interacting clones, the PCR-amplified pACT2 inserts were sequenced using standard techniques. The identity of the inserts was determined by comparing the cDNA sequences with those deposited in GenBank®.

Yeast two-hybrid one-on-one interactions

To demonstrate the specificity of the interaction between the ALP C-terminus and the MC4-R C-terminus, one-on-one two-hybrid analyses were performed to compare the interaction potential of the ALP C-terminus and the attractin C-terminus with the MC4-R C-terminus. The vectors containing the yeast GAL4 binding domain (pGBKT7) with or without the insert for the C-terminal domain of ALP or attractin were transformed individually into yeast strain Y187. The vector containing the GAL4 activation domain (pACT2) fused with the C-terminal domain of MC4-R was transformed into yeast strain AH109. The yeast strains were then mated as described in the manufacturer's (Clontech) protocol and co-transformants were selected. The MC4-R C-terminus was also assayed for activation function in the presence of a bait vector without an insert, and the bait vector was assayed for activation function in the absence of the library vector, eliminating more false positives. A control bait vector containing lamin C was also used to ensure that the library vector caused specific activation only in the presence of a bait vector containing the MC4-R C-terminus. Positive interactions were detected and analysed as described above.

N- and C-terminally truncated constructs of ALP and MC4-R

N- and C-terminally truncated constructs were made by PCR amplification using the C-terminal cDNAs of mouse ALP and mouse MC4-R subcloned into the pGEX-2T vector (Amersham Pharmacia Biotech, Piscataway, NJ, U.S.A.). Amplified fragments were cloned in the pGEX-2T vector in-frame with the GST (glutathione S-transferase) gene. All DNA sequences were confirmed by sequencing.

Expression of GST and MBP (maltose-binding protein) fusion proteins, and *in vitro* binding assays

The C-terminal region of the MC4-R protein (residues 303–332) and the C-terminal region of the ALP protein (the final 110 amino acids) were subcloned in-frame with the GST gene into the pGEX-2T vector, and in-frame with the MBP gene into a modified pMAL-ce vector (New England Biolabs, Beverly, MA, U.S.A.) containing a T7 tag. In addition, a set of deletion constructs in the C-terminal portions of the ALP and MC4-R proteins subcloned into the pGEX-2T vector were prepared for use in mapping of the interaction domain between ALP and MC4-R. Recombinant GST-fusion proteins were synthesized in BL-21 *Escherichia coli* bacteria and purified on glutathione–Sepharose resin under non-denaturing conditions. BL-21 cultures were induced with 0.4 mM IPTG (isopropyl β-D-thiogalactoside) for 3 h at 30 °C. Bacteria were harvested and pellets were resuspended in ice-cold PBS containing 1 % Triton X-100, 1 mM EDTA, 1 mM dithiothreitol and protease inhibitors (Complete EDTA-free; Roche) and then lysed by sonication in short pulses of 15 s. Cell debris was removed by centrifugation at 9000 ***g*** for 20 min at 4 °C. The resultant supernatant was incubated with glutathione–Sepharose beads (50 % slurry) (Sigma) for 2.5 h at 4 °C. The beads were washed four times in the same buffer as before and then applied to a glutathione–Sepharose column equilibrated with PBS. Elution was performed with 10 mM GSH in 50 mM Tris, pH 7.5. GST protein fractions were dialysed for 4 h in dialysis buffer (20 mM Hepes, 100 mM NaCl, 0.5 mM EDTA, 10 % glycerol, 1 mM dithiothreitol and 0.2 mM PMSF) at 4 °C. Cultures of *E. coli* DH5-α containing pMAL-T7-MC4-R(C-terminus) and pMAL-T7-ALP(C-terminus) plasmids were induced with

0.3 mM IPTG for 3 h at 30 °C. Bacteria were harvested and pellets were resuspended in ice-cold column buffer (20 mM Tris/HCl, pH 7.4, 200 mM NaCl and 1 mM EDTA, pH 8.0) and sonicated. Cell debris was then removed by centrifugation at 9000 ***g*** for 20 min at 4 °C. The cleared supernatants were incubated with amylose resin (New England Biolabs) and eluted with column buffer plus 10 mM maltose. GST and MBP fusion proteins were analysed by SDS/PAGE before use in the assay.

For the *in vitro* binding assays, GST-fusion proteins [GST–(ALP C-terminus) or GST–(MC4-R C-terminus) constructs] were incubated with 20 μl of glutathione–Sepharose beads (50 % slurry; Pharmacia) in 300 μl of ice-cold binding buffer (20 mM Hepes, pH 7.8, 10 % glycerol, 0.1 mM EDTA, pH 8.0, and 100 mM KCl) overnight at 4 °C. After three washes with the same ice-cold buffer, the MBP-fusion proteins [MBP–(MC4-R C-terminus) or MBP–(ALP C-terminus)] were incubated with the GST fusion proteins for 2 h at 4 °C and then washed eight times with 500 μl of the same buffer at room temperature. GST alone was used as a negative control. SDS/PAGE loading buffer was used to release the bound MBP-fusion proteins. Samples were loaded on to an SDS/PAGE gel and transferred on to a PVDF membrane for Western-blot analysis with an antibody against the T7 tag (Novagen, Madison, WI, U.S.A.).

RT-PCR (reverse transcription–PCR)

A Mouse Multiple Tissue cDNA panel (Clontech) was used, which consisted of cDNA preparations of 7-day embryo, 11-day embryo, 15-day embryo and 17-day embryo samples. As a control, 3 μl of each cDNA preparation was tested using G3PDH (glyceraldehyde-3-phosphate dehydrogenase) control primers to amplify a single 1 kb band in 25 cycles of PCR. Following this, 5 μl portions of the cDNAs were amplified by PCR in a DNA thermal cycler (PerkinElmer Corp., Foster City, CA, U.S.A.) using the *Taq* DNA polymerase (Fermentas Life Sciences). PCR conditions were: 94 °C for 3 min, then 30 cycles of 94 °C/45 s, 57 °C/45 s and 72 °C/1 min, followed by a final extension at 72 °C using primers designed specifically for ALP (5′, AACACAATCATGGATCTCGTCCAGTTCTTTGTC; 3′, TCAGACACAAGTTCCTTGACGTGTGGAGAG), corresponding to the transmembrane domain and the intracellular part of the molecule. The PCR products were resolved and visualized by electrophoresis through a 1 % (w/v) agarose/ethidium bromide gel.

Northern blot analysis

Mouse multiple tissue Northern blot filters containing 2 μg of poly(A)$^+$ (polyadenylated RNA) were purchased from Clontech. A cDNA probe of ALP was made from a 3 kb purified PCR product from the activation domain insert of a positive yeast clone. A β-actin control probe was supplied by Clontech. The probes were labelled with [α-^{32}P]dCTP using the *rediprimeII* random prime labelling system (Amersham) to give probes of high specific radioactivity ($>1\times10^9$ d.p.m./μg). Hybridization and washing were performed according to standard procedures. The resulting signals were visualized by standard autoradiography.

Animals and histology

Animals included C56BL/6J mice (female, 20–30 g; Jackson Laboratory, Bar Harbor, ME, U.S.A.) and CBA/C56BL/6J F1 transgenic mice, in which GFP (green fluorescent protein) is produced under the control of the MC4-R promoter [23]. These mice were housed, with food and water available *ad libitum*, in a light-controlled (12 h on/12 h off; lights on 07:00 h) and temperature-controlled (21.5–22.5 °C) environment. The animals and procedures used in this study were in accordance with the guidelines and approval of the Harvard Medical School and Beth Israel Deaconess Medical Center Institutional Animal Care and Use Committees, and the guidelines of The Rockefeller Animal Research Center. Mice were deeply anaesthetized with an intraperitoneal injection of chloral hydrate (350 mg/kg) and perfused transcardially with DEPC (diethyl pyrocarbonate)-treated 0.9 % NaCl, followed by 500 ml of 10 % neutral buffered formalin. Brains were removed, stored in the same fixative for 4 h at 4 °C, immersed in 20 % sucrose in DEPC-treated PBS at 4 °C overnight, and cut coronally into 25 μm slices into 1:5 equal series on a freezing microtome. Sections were stored at -20 °C in an antifreeze solution [24] until sections were treated for ISHH (*in situ* hybridization histochemistry; see below) coupled or not with immunohistochemistry.

Generation of an ALP cRNA probe

The sequence encoding the final 110 amino acids of the ALP gene was subcloned into a pBKS(+) vector using *Eco*RI/*Xho*I restriction sites. To generate antisense ^{35}S-labelled cRNA, the plasmids were linearized by digestion with *Eco*RI and subjected to *in vitro* transcription with T3 RNA polymerase as described in the manufacturer's (Promega) protocol. For generation of sense ^{35}S-labelled cRNA, the plasmids were linearized by digestion with *Xho*I and subjected to *in vitro* transcription with T7 RNA polymerase according to the manufacturer's protocol.

ISHH

Single-label ISHH for ALP mRNA was performed as reported previously [17,25]. Tissue sections were mounted on to Super-Frost slides (Fisher Scientific, Pittsburgh, PA, U.S.A.), air-dried, and stored in desiccated boxes at -20 °C. Prior to hybridization, sections were fixed in 4 % formaldehyde in DEPC-treated PBS (pH 7.0) for 20 min at 4 °C, dehydrated in ascending concentrations of ethanol, cleared in xylenes for 15 min, rehydrated in descending concentrations of ethanol, and placed in pre-warmed sodium citrate buffer (95–100 °C, pH 6.0). Slides were then placed in a Sharp (Nahwah, NJ, U.S.A.) R-510C commercial microwave oven (1100 W) for 10 min at 70 % power (temperature 95–100 °C), dehydrated in ascending concentrations of ethanol, and air-dried. The ^{35}S-labelled cRNA probe for ALP mRNA was then diluted to 10^6 c.p.m./ml in a hybridization solution composed of 50 % formamide, 10 mM Tris/HCl, pH 8.0, 5.0 mg of tRNA (Boehringer-Mannheim, Indianapolis, IN, U.S.A.), 10 mM dithiothreitol, 10 % dextran sulphate, 0.3 M NaCl, 1 mM EDTA, pH 8.0, and 1 × Denhardt's solution (Sigma). Hybridization solution and a coverslip were applied to each slide, and sections were incubated for 12–16 h at 57 °C. Coverslips were then removed and slides washed with 2 × SSC (1 × SSC is 0.15 M NaCl/0.015 M sodium citrate, pH 7.0). Sections were then incubated in 0.002 % RNAase A (Boehringer-Mannheim) with 0.5 M NaCl, 10 mM Tris/HCl, pH 8.0, and 1 mM EDTA for 30 min. Subsequently, sections were washed in decreasing concentrations of SSC containing 0.25 % dithiothreitol: 2 × SSC at 50 °C for 1 h, 0.2 × SSC at 55 °C for 1 h, and 0.2 × SSC at 60 °C for 1 h. Sections were next dehydrated in graded ethanol (50 %, 70 %, 80 % and 90 %) containing 0.3 M sodium acetate, followed by 100 % ethanol. Slides were air-dried and placed in X-ray film cassettes with BMR-2 film (Kodak, Rochester, NY, U.S.A.) for 2–3 days. Slides were then dipped in NTB2

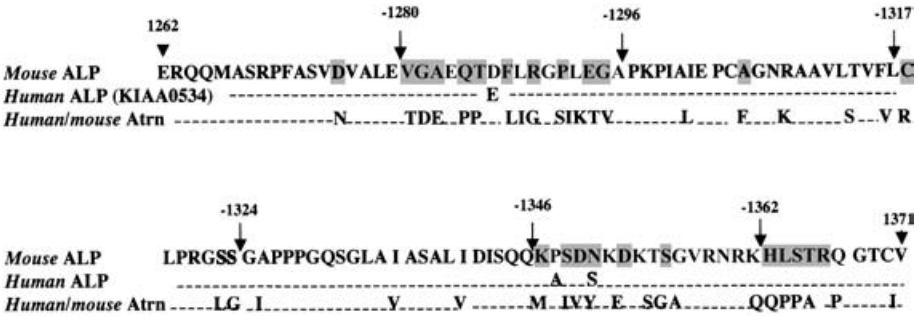

Figure 1 Sequence alignment of the C-terminal parts of mouse and human ALPs and human and mouse attractin (Atrn) proteins

The mouse ALP amino acid sequence reported here corresponds to the positive cDNA sequence in the yeast two-hybrid screen. Dashes correspond to amino acid identities. Non-conservative amino acid changes relative to the attractin sequence are boxed in grey. The positions of ALP C-terminal deletions are reported above the ALP sequence, and were designed based on differences from the attractin sequence. The numbers refer to amino acid residues in the full-length ALP protein.

photographic emulsion (Kodak), dried, and stored in desiccated and foil-wrapped boxes at 4 °C for 3–4 weeks. Finally, slides were developed with D-19 developer (Kodak), conterstained with thionin, dehydrated in graded ethanols, cleared in xylenes, and coverslips were added using Permaslip. Control experiments to confirm the specificity of this protocol included hybridization with sense probes and with antisense probes after treatment with RNAase A (200 μg/ml). In one animal, an adjacent series of sections was stained with thionin to identify nuclear boundaries [17,25].

Dual-label ISHH/immunohistochemistry

To detect MC4-R-positive cells co-expressing ALP mRNA, we used a transgenic mouse line in which GFP is produced under the control of the MC4-R promoter (MC4-R/GFP mouse) [25]. For this purpose, immunohistochemistry was coupled with free-floating ISHH [23,26]. Brain sections were first rinsed in DEPC-treated PBS (pH 7.0) and then pretreated with 1 % sodium borohydride (Sigma) in DEPC-PBS for 15 min at room temperature. After washing in DEPC-PBS, sections were rinsed in 0.1 M triethanolamine (pH 8.0) and incubated in 0.25 % acetic anhydride in 0.1 M triethanolamine for 10 min. After washing in 2 × SSC, sections were incubated in the above-mentioned hybridization solution containing the MC4-R probes diluted to 10^6 c.p.m./ml for 12–16 h at 57 °C. Subsequently, sections were rinsed in 4 × SSC and incubated in 0.002 % RNAase A (Roche Molecular Biochemicals) with 0.5 M NaCl, 10 mM Tris/HCl, pH 8, and 1 mM EDTA for 30 min at 37 °C. Sections were rinsed with 2 × SSC and then with 50 % formamide in 0.2 × SSC at 50 °C. Subsequently, sections were washed in decreasing concentrations of SSC: 2 × SSC at 50 °C for 1 h, 0.2 × SSC at 55 °C for 1 h, and 0.2 × SSC at 60 °C for 1 h. After washing in PBS (pH 7.4), immunohistochemistry for GFP was performed as described previously, using standard peroxidase immunohistochemical methods and diaminobenzidine as the chromogen [26]. Sections were mounted on to SuperFrost slides (Fisher Scientific), and were placed in X-ray film cassettes with BMR-2 film (Kodak) for 2–3 days. Slides were then treated as described above without counterstaining.

The following method of scoring double-labelled cells was employed [27]. The hybridization was defined as positive if the number of silver grains accumulated was 5-fold above background levels. Estimates of background hybridization levels were made by calculating the mean number of silver grains overlying a counting grid (100 mm^2) in the internal capsule. Cells were defined as double-labelled if the silver grains were scattered conforming to the shape of cell bodies showing both positive hybridization and GFP immunoreactivity.

Anatomical analysis and production of photomicrographs

Sections were analysed with a Zeiss Axioskop or a Zeiss Stemi 2000-C dissecting microscope. Cytoarchitectonic details were added by using a camera lucida. Photomicrographs were produced with a Spot digital camera (Diagnostic Instruments, Sterling Heights, MI, U.S.A.) attached to the microscopes and an Apple Macintosh G3 computer. Image editing software (Adobe Photoshop 5.5) was used to combine microphotographs on to plates, and figures were printed on a dye sublimination printer (Kodak 8670 PS). Only the contrast and brightness were adjusted.

RESULTS

Identification of ALP as an MC4-R-interacting protein using the yeast two-hybrid assay

In order to characterize binding partners of the MC4-R, the C-terminal region of the MC4-R (residues 303–332) was used as bait in a yeast two-hybrid screen. A screen of a mouse brain library resulted in 30 colonies that tested positive on the basis of growth on selective media (SD/ – Ade/ – His/ – Leu/ – Trp), as well as induction of *lacZ* expression causing a blue colour when assayed with X-galactosidase. Nucleotide analysis of the positive clones revealed one EST (expressed sequence tag) that predicted the C-terminus of a protein that is 63 % similar in amino acid structure to mouse attractin (Figure 1). This protein was named ALP. Repeat one-on-one yeast two-hybrid analyses were performed to compare the interaction potential of the C-termini of ALP and attractin with the MC4-R C-terminus. It was found that only the ALP C-terminus was able to interact directly with the MC4-R C-terminus; the attractin C-terminus did not interact directly with the MC4-R C-terminus.

GST pull-down assay confirms the two-hybrid result, showing a direct interaction between MC4-R and ALP

In order to confirm biochemically the interaction between mouse MC4-R and mouse ALP initially found using the yeast two-hybrid assay, the C-termini of MC4-R and ALP were fused in-frame

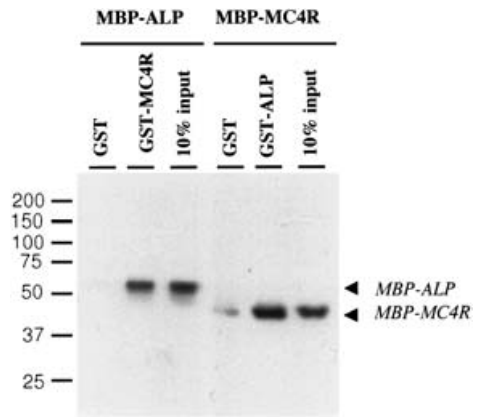

Figure 2 Direct interaction between the C-terminal tails of mouse MC4-R and mouse ALP demonstrated by GST pull-down assays

The bacterial fusion proteins MBP–ALP, MBP–MC4-R, GST–ALP and GST–MC4-R were produced as described in the Experimental section and used in GST pull-down assays to confirm the interaction observed in the yeast two-hybrid screen. Bound MBP-fusion proteins were detected by using an anti-T7 antibody and revealed by enhanced chemiluminescence detection. GST alone was used as a negative control. The arrows indicate the positions of MBP–ALP and MBP–MC4-R C-terminal proteins. Portions of 10 % of MBP-fusion proteins used in the pull-down assays were loaded as input (10 % input).

with both the GST and the MBP genes and used in GST pull-down assays. As shown in Figure 2, the MBP–ALP protein interacted specifically with the GST–MC4-R construct, which was confirmed by the reverse experiment. These results indicate that the interaction between the C-termini of these proteins is direct.

Mapping of the regions of ALP and MC4-R that interact with each other

Eight truncated fragments of the mouse ALP C-terminal domain, designed based on conservation of sequence between ALP and attractin, were tested in GST pull-down assays for their ability to bind the MC4-R C-terminus directly. The results of this C-terminal deletion mapping narrowed down the critical interacting domain of ALP to the region encoded by amino acids 1280–1317 (Figure 3). The same approach was used to define more precisely the region in the MC4-R C-terminal tail that interacts with ALP. Four deleted constructs of this C-terminal part of MC4-R were tested in GST pull-down assays with the MBP–(ALP C-terminus) fusion protein. The mouse MC4-R ($-326/-319/-313$) constructs still bound specifically to the MBP-(ALP C-terminus) protein. However, when amino acids 303–313 were deleted, as in the mouse MC4-R C-terminus ($+313$) construct, the binding was lost, demonstrating that this part of the MC4-R C-terminus is required for the interaction between the C-termini of MC4-R and ALP (Figure 4).

Pattern of expression of ALP

Northern blot analysis was performed in order to determine the tissue distribution and size of mRNA transcripts encoding the ALP cDNA. Poly(A)$^+$ RNA from mouse tissues (2 μg/lane) was probed with a 3 kb cDNA probe specific for ALP. A β-actin probe is shown as a positive control (Figure 5). ALP expression was seen at high levels in the brain, kidney, heart, lung and liver, and at low levels in the spleen, skeletal muscle and testis, by Northern blot analysis. The size of the major transcript was 8.5 kb. A minor transcript of 4.4 kb was also seen in the heart, brain,

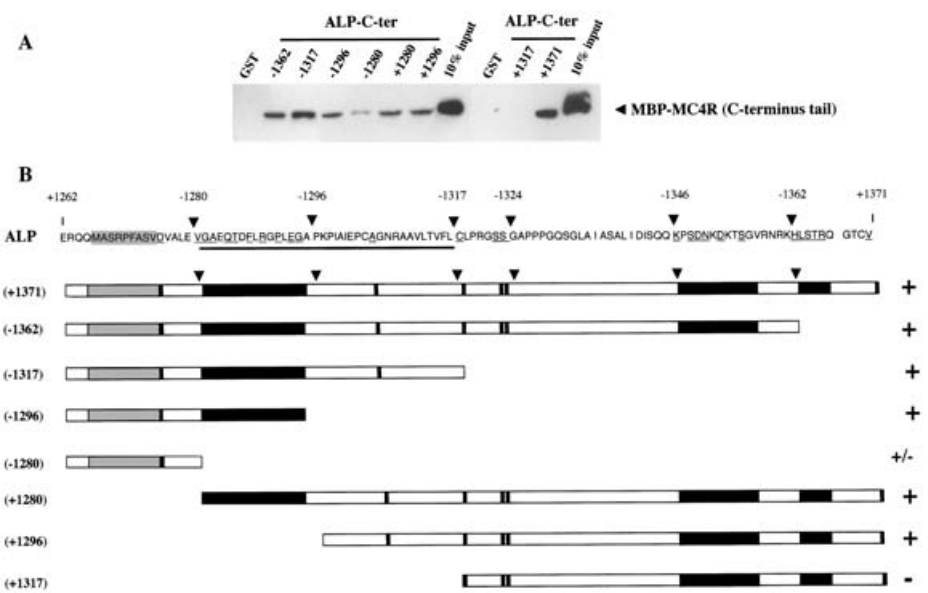

Figure 3 *In vitro* mapping by GST pull-down assays of the part of the ALP domain that interacts with the MC4-R C-terminal tail

Nine deletion constructs of the ALP C-terminal tail (ALP C-ter) fused to GST were used to pull down the MC4-R C-terminal tail fused to MBP–T7 tag protein. (**A**) *In vitro* binding assay testing the ability of seven deletion constructs of the C-terminus of ALP to bind the MBP–(MC4-R C-terminal tail) fusion protein. Bound proteins were detected by using an anti-T7 antibody and revealed by enhanced chemiluminescence detection. Numbers correspond to the ALP truncated fragments. GST alone and ALP C-ter ($+1371$) were used as negative and positive controls respectively. The arrowhead indicates the position of the MBP–(MC4-R C-terminal tail) fusion protein. (**B**) The ALP amino acid sequence is reported, including the highly conserved MASRFASV motif (grey box) and amino acid changes in charge compared with the mouse attractin protein sequence, which are underlined and represented by darkly shaded boxes in the scheme below. The deletions made are noted above the ALP sequence. Construct binding is indicated on the right of the diagram: $+$, interaction; $-$, no interaction; $+/-$, weak interaction. The domain of ALP required for interaction with the C-terminus of MC4-R is underlined. Portions of 10 % of the MBP–(MC4-R C-terminal tail) fusion protein used in the pull-down assays were loaded as input (10 % input).

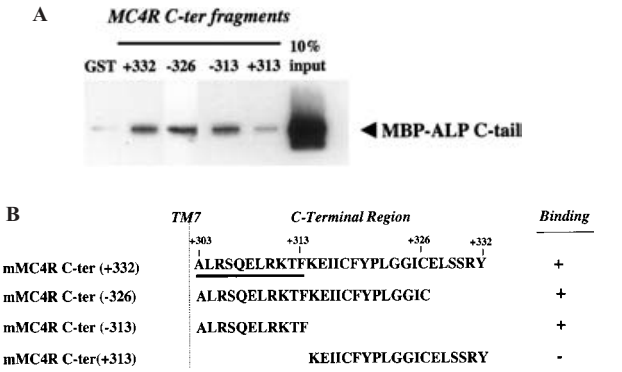

Figure 4 ***In vitro*** **mapping of the MC4-R domain that interacts with the ALP C-terminal tail**

Four GST–(MC4-R C-terminal tail) deletion constructs were assessed for binding to the MBP–(ALP C-terminal tail) protein (**A**) Three of four deleted constructs of the MC4-R C-terminus (MC4-R C-ter) fused to GST protein are shown. GST and MC4-R C-ter (+ 332) were used as negative and positive controls respectively. MC4-R C-ter (− 326) and (− 313) constructs pull down the ALP C-terminal tail fused to MBP–T7 tag protein, whereas MC4-R C-ter (+ 313) does not. Bound proteins were detected by using an anti-T7 antibody and revealed by enhanced chemiluminescence detection. The position of the MBP–(ALP C-terminal tail) protein is indicated by an arrowhead. (**B**) MC4-R C-terminus construct sequences used in *in vitro* binding assays are reported, and the domain of MC4-R required for the interaction with the C-terminus of ALP is boxed. TM7, transmembrane domain 7. Construct binding is indicated on the right: +, interaction; −, no interaction. Portions of 10 % of MBP–(ALP C-terminal tail) protein used in the pull-down assay were loaded as input (10 % input).

liver and lung, another minor transcript of 5 kb was seen only in the liver, and a further minor transcript of 5.4 kb was specific to the testis. Moreover, as shown by RT-PCR (Figure 5B), ALP was also expressed at the 7-day embryonic stage and maintained during development. The G3PDH PCR shows that samples were normalized.

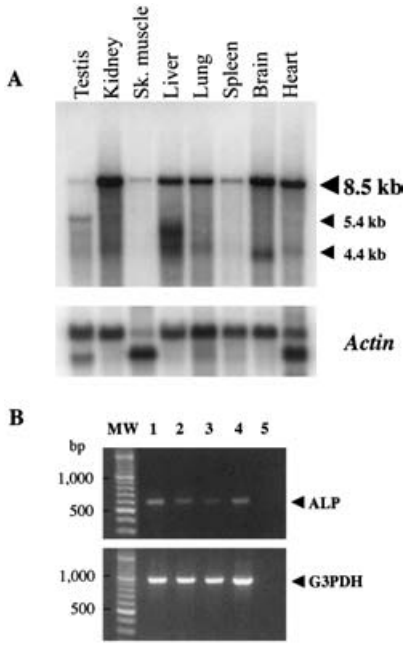

Figure 5 Tissue expression patterns of ALP transcripts

(**A**) Northern hybridization to mRNA from indicated tissues (2 μg/lane) using a probe containing the mouse ALP cDNA fragment (intracellular C-terminal part of ALP and 3′ non-coding sequence) detected a major 8.5 kb transcript that was highly expressed in kidney, liver, lung, brain and heart, and three minor shorter transcripts of 5.4 kb, 5 kb and 4.4 kb in testis, liver and brain, heart, liver and lung. Mouse actin was used as an internal control. Arrowheads indicate ALP transcripts. Sk, skeletal. (**B**) PCR on a mouse Multiple Tissue cDNA panel I (Clontech). Upper panel: primers for ALP were used in 30 cycles of PCR to amplify a 500 bp fragment corresponding to the transmembrane domain and intracellular part of ALP. Lower panel: primers for G3PDH were used in 25 cycles of PCR to amplify a 923 bp fragment as control of cDNA normalization. Lanes 1, 7-day embryo; lanes 2, 11-day embryo; lanes 3, 15-day embryo; lanes 4, 17-day embryo; lanes 5, negative control without cDNA; lanes MW, 100 bp DNA ladder.

Neuronal cellular localization of ALP and co-localization with MC4-R

Hybridization for ALP was widespread in the mouse brain (Table 1 and Figure 6). The description of ALP expression sites uses the nomenclature in the mouse brain atlas of Franklin and Paxinos [27a]. As referenced in Table 1, ALP mRNA was assessed as highest density, high density, moderate density and low density to describe the level of hybridization. Both the strength of the hybridization signal per cell and the number of labelled cells in a given area were considered in the scoring of hybridization.

The specificity of ALP hybridization was tested using standard sense hybridization and antisense hybridization with RNase pretreatment. Both control experiments revealed extremely faint hybridization in the piriform cortex, dentate gyrus, and fields CA1–CA3 of the hippocampal formation. After RNase pretreatment, weak antisense hybridization was also seen in the reticular nucleus of the thalamus. In tissue not pretreated with RNAase, however, these sites displayed high levels of antisense ALP hybridization. Thus ALP mRNA expression cannot be excluded in these brain regions, and region-specific RT-PCR experiments are required to address this issue.

ALP mRNA expression was observed in many of the mouse brain sites that have been reported to express MC4-R mRNA [23], as shown in Table 1 and Figure 6. By using the MC4-R/GFP mice, we also detected MC4-R-positive cells co-expressing ALP mRNA (Table 1). The dual-labelled cells were widely distributed in the neocortical (Figure 7A) and hippocampal (Figure 7B) regions. Within the amygdala, an aggregation of GFP-immunoreactive cells co-expressing ALP mRNA was observed in the nucleus of the lateral olfactory tract (Figure 7C) and the basolateral amygdaloid nucleus (Figure 7D). Notably, within the hypothalamus, the paraventricular nucleus (Figures 7E and 7F) and the perifornical area (Figure 7G, H) contained GFP-immunoreactive cells showing ALP hybridization. Dual-labelled cells were sparse in the pedunculopontine tegmental nucleus (Figure 7I) and dense in the DMV (dorsal motor nucleus of the vagus) (Figures 7J and 7K). Interestingly, most of the MC4-R-positive cells of the DMV expressed ALP. Double labelling was also evident in the pontine reticular and gigantocellular (Figure 7L) reticular nuclei.

DISCUSSION

A yeast two-hybrid screen has identified the C-terminus of ALP as a protein domain that interacts directly with the C-terminus of the MC4-R. These findings were confirmed *in vitro* by GST pull-down assays. N- and C-terminal deletion studies have shown that amino acids 1280–1317 of the C-terminus of mouse ALP are required for the binding of mouse MC4-R, and that residues 303–313 in the MC4-R intracellular C-terminal tail are involved in the binding of the ALP C-terminal fragment. Moreover, this interaction seems highly specific, because the C-terminus of ALP was not able to pull down the C-terminus of the β_2-adrenergic receptor used as a G-protein-coupled receptor heterologous sequence (a gift from Dr Duane D. Hall, Department of Pharmacology, University of Wisconsin, Madison, WI, U.S.A.; results not shown). Furthermore, the ALP-binding motif contains a Thr

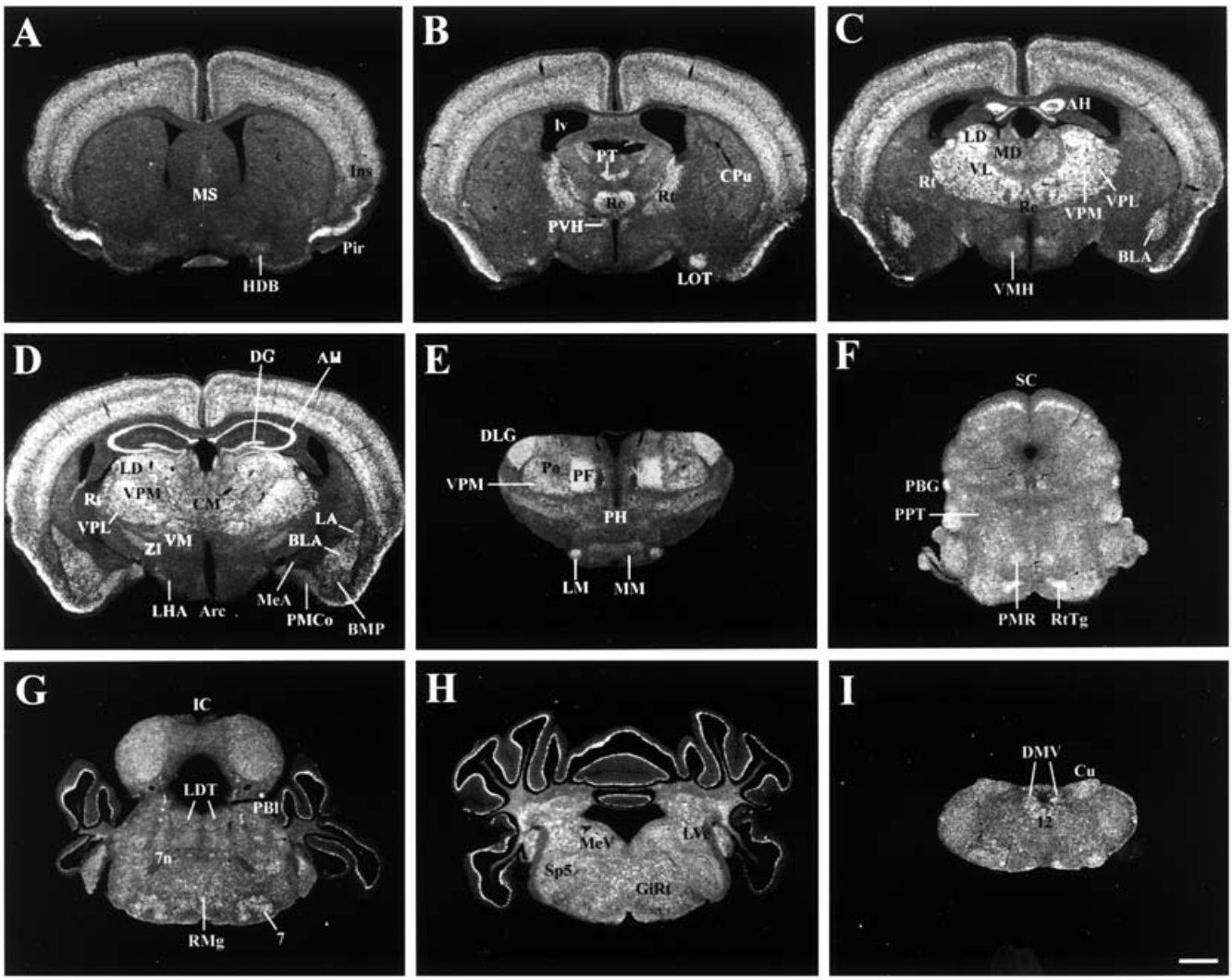

Figure 6 ***In situ*** **hybridization analysis showing expression of ALP in adult mouse brain**

A series of low-power photomicrographs summarizing ALP mRNA expression across the mouse brain. ALP-specific hybridization is evident in brain sites involved in maintaining energy homoeostasis, e.g. the arcuate (Arc), paraventricular (PVH) and ventromedial (VMH) nuclei of the hypothalamus, the lateral hypothalamic area (LHA), the lateral parabrachial nucleus (PBl) and the DMV. Moderate-to-high levels of ALP mRNA expression are also seen in the cortical, thalamic and brainstem regions. Abbreviations: AH, Ammon's horn; BLA, basolateral nucleus of the amygdala, anterior part; BMP, basomedial nucleus of the amygdala, posterior part; CM, central medial nucleus; CPu, caudate-putamen; Cu, cuneate nucleus; DG, dentate gyrus; DLG, dorsal geniculate nucleus; DTg, dorsal tegmental nucleus; GiRt, gigantocellular reticular nucleus; Hb, habenular nucleus; HDB, horizontal limb of the diagonal band of Broca; IC, inferior colliculus; Ins, insular cortex; LA, lateral nucleus of the amygdala; LD, laterodorsal nucleus of the thalamus; LDT, laterodorsal tegmental nucleus; LM, lateral mammillary nucleus; LOT, nucleus of the lateral olfactory tract; lv, lateral ventricle; LVe, lateral vestibular nucleus; MD, mediodorsal nucleus; MeA, medial nucleus of the amygdala; MM, medial mammillary nucleus; MS, medial septum; MeV, medial vestibular nucleus; PBG, parabigeminal nucleus; PF, parafascicular nucleus of the thalamus; PH, posterior hypothalamic area; Pir, piriform cortex; PMCo, cortical nucleus of the amygdala, posteromedial part; PMR, paramedial raphe; PnRt, pontine reticular nucleus; Po, posterior thalamic nuclear group; PPT, pedunculopontine tegmental nucleus; PT, paratenial nucleus; Re, nucleus reuniens of the thalamus; RMg, raphe magnus; Rt, reticular nucleus of the thalamus; RtTg, reticular tegmental nucleus; SC, superior colliculus; Sp5, spinal trigeminal nucleus; VL, ventrolateral nucleus; VM, ventromedial nucleus of the thalamus; VPL, ventral posterolateral nucleus; VPM, ventral posteromedial nucleus; ZI, zona incerta; 7, facial nucleus; 7n, facial nerve; 12, hypoglossal nucleus. Scale bar = 1 mm.

residue (position 312) in the MC4-R intracellular C-terminal tail which has been recently characterized as a potential site for phosphorylation by protein kinase A and which plays a role in the internalization of MC4-R by agonist [28], suggesting a potential role of ALP in the trafficking of MC4-R.

Tissue distribution analysis revealed that mouse ALP and its homologue, attractin, share a broad expression pattern. A high level of ALP mRNA was seen in brain, kidney, heart, lung and liver, similar to attractin [29]. ALP expression was also seen in 7-day mouse embryos by RT-PCR, indicating that the expression of this protein occurs at an early stage. Several ALP transcripts were detected: a major transcript of 8.5 kb and other shorter minor transcripts. The C-terminal ALP probe is able to recognize shorter transcripts, suggesting these cannot encode an alternative N-terminal soluble isoform as is observed for attractin [30]. A 3′ RACE (rapid amplification of cDNA ends) PCR performed on a mouse brain cDNA library has shown that two polyadenylation sites are used, suggesting that the 4 kb transcript in brain and possibly in other tissues, might correspond to the use of the proximal polyadenylation site (results not shown).

In the present study we have demonstrated widespread ALP hybridization in the mouse brain (Figure 6). ALP mRNA is expressed in many regions of the brain that overlap with those that express attractin mRNA, such as the cortex, hippocampus, cerebellum and midbrain [22]. However, there are some differences, as ALP seems to be more highly expressed in the entorhiral cortex, cingulate

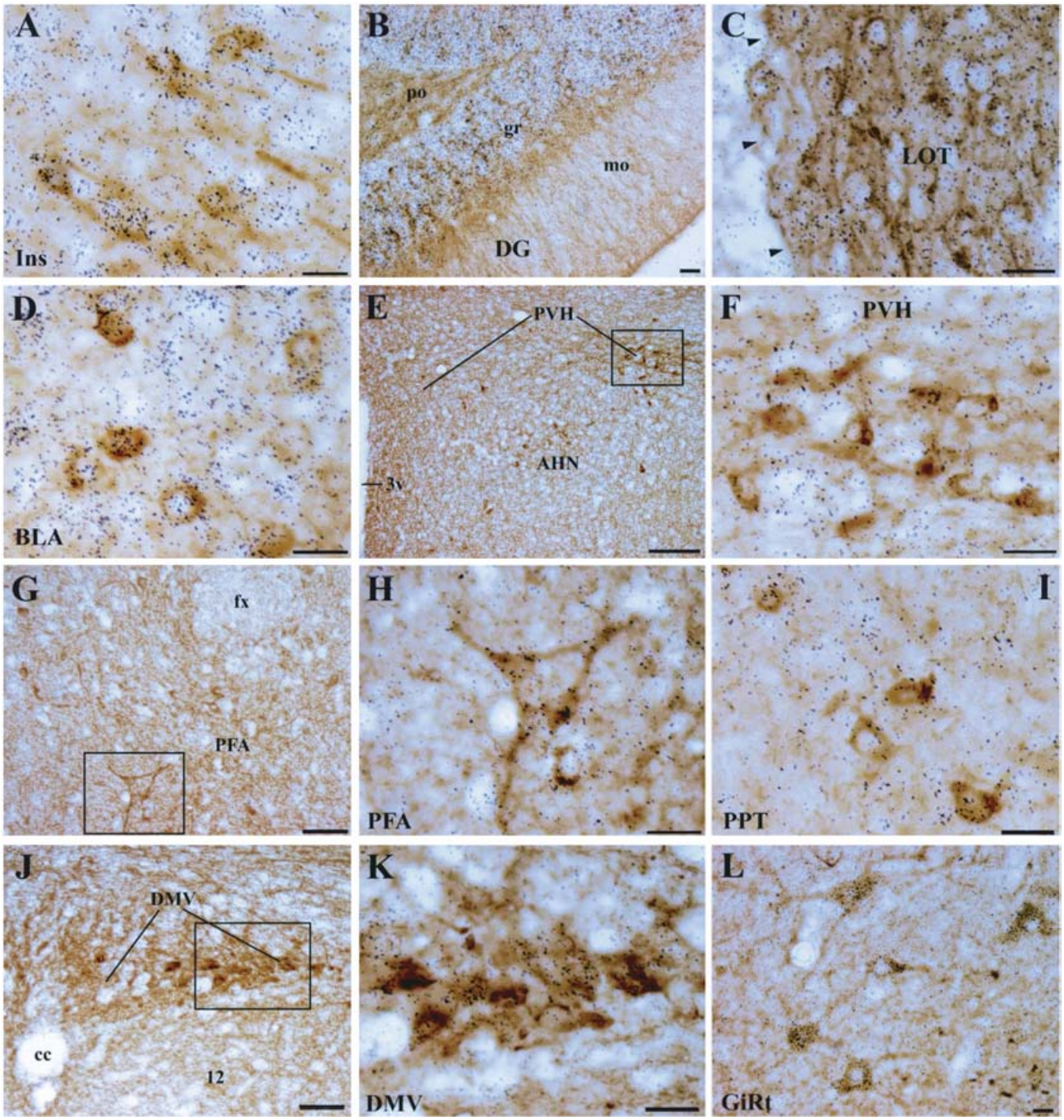

Figure 7 Co-localization studies showing overlap of ALP and MC4-R expression in the mouse

A series of photomicrographs showing ALP mRNA expression (grain accumulation) in GFP-immunoreactive (i.e. MC4-R-positive) cells (brown cytoplasm). Note the presence of dual-labelled cells in feeding-regulatory brain sites, including the paraventricular nucleus of the hypothalamus (PVH; **E**, **F**), the perifornical area (PFA; **G**, **H**) and the DMV (**J**, **K**). Dual-labelled cells are also distributed in the insular cortex (Ins; **A**), dentate gyrus (DG; **B**), nucleus of the lateral olfactory tract (LOT; **C**), basolateral nucleus of the amygdala (BLA; **D**), pedunculopontine tegmental nucleus (PPT; **I**), and gigantocellular reticular nucleus (GiRt; **L**). Abbreviations: cc, central canal; fx, fornix; gr, granular layer; mo, molecular layer; po, polymorphic layer; 3v, third ventricle; 12, hypoglossal nucleus; AHN, anterior hypothalamic nucleus. Arrowheads in (**C**) indicate the medial border of the LOT. Scale bars = 20 mm in (**A**)–(**D**), (**F**), (**H**), (**I**), (**K**) and (**L**), 100 mm in (**E**), and 50 mm in (**G**) and (**J**).

area and anterior limbic cortex in forebrain, in the thalamus and in the amygdala than attractin, and expressed to a lesser extent in olfactory tubercle and lateral septum or in CA1 and CA3 pyramidal layers of hippocampus, for instance.

By using MC4-R/GFP mice, we also observed MC4-R-positive cells co-expressing ALP mRNA in several autonomic control sites involved in maintaining energy homoeostasis. In the paraventricular nucleus of the hypothalamus, for example, dual-labelled cells were present in the most lateral portion of the posterior division (Figures 7E and 7F). The posterior part of this region contains neurons projecting to both parasympathetic and sympathetic preganglionic neurons in the DMV and spinal cord

Table 1 ALP mRNA expression in the mouse brain

Qualitative estimates of ALP mRNA expression were made by considering both signal strength and the number of labelled cells, as described in the Results section. The following six-point density scale was used: ++++, highest density; +++, high density; ++, moderate density; +, low density above background; ±, very low and inconsistent density; −, background density. Asterisks (*) denote the mouse brain sites that have been reported to express MC4-R mRNA [16,23]. Daggers (†) denote the brain sites where MC4-R-positive cells co-expressing ALP mRNA were observed.

Region	Expression
Cerebral cortex	
Auditory cortex, dorsal*†	+++
Auditory cortex, primary*†	+++
Auditory cortex, ventral*†	+++
Cingulate cortex*†	+++
Dorsal peduncular cortex*	+++
Ectorhinal cortex*†	+++
Entorhinal cortex, lateral*†	+++
Entorhinal cortex, medial*	+++
Infralimbic cortex*	+++
Insular cortex, agranular*†	+++
Insular cortex, granular*†	+++
Motor cortex, primary*†	+++
Motor cortex, secondary*†	+++
Olfactory tubercle*	+
Orbital cortex*	++
Parietal association area*†	+++
Perirhinal cortex*†	+++
Piriform cortex*†	++++
Prelimbic cortex*	+++
Retrosplenial cortex*†	+++
Somatosensory area*†	+++
Temporal association area*†	+++
Visual cortex, primary*†	+++
Visual cortex, secondary*†	+++
Cerebellum	
Cortex (Purkinje cell layer)	+++
Lateral cerebellar nucleus	++
Striatum	
Caudoputamen*†	+
Globus pallidus	+
Nucleus accumbens, shell*	±
Nucleus accumbens, core*	±
Substantia nigra, compact part	+
Substantia nigra, lateral part	+
Substantia nigra, reticular	+
Subthalamic nucleus	+
Hippocampus and septum	
Ammon's horn, CA1 (pyramidal layer)* †	++
Ammon's horn, CA2 (pyramidal layer)* †	++++
Ammon's horn, CA3 (pyramidal layer)* †	+++
Dentate gyrus (granular layer)* †	++
Induseum griseum	+++
Lateral septal nucleus, dorsal*†	+
Medial septal nucleus*	+
Nucleus of the diagonal band*	+
Parasubiculum	+++
Presubiculum	+++
Subiculum, dorsal	+++
Subiculum, intermediate*†	+++
Subiculum, ventral*†	+++
Amygdala	
Amygdalohippocampal transitional area*	++
Amygdalopiriform transition area	+++
Anterior amygdaloid area*†	+
Basolateral nucleus, anterior*†	+++
Basolateral nucleus, posterior*†	+++
Basomedial nucleus, anterior*†	++
Basomedial nucleus, posterior*	++
Central nucleus, capsular	±
Central nucleus, lateral*	+
Central nucleus, medial*†	+
Cortical nucleus, posterior*	++
Lateral nucleus*	++
Medial nucleus, anterior*†	+
Medial nucleus, posterior*†	++
Nucleus of the lateral olfactory tract*†	++++
Substantia innominata*	+
Thalamus	
Angular nucleus	+
Anterodorsal nucleus	++
Anteromedial nucleus	+
Anteroventral nucleus	+
Central lateral nucleus	+
Central medial nucleus	+
Interanterodorsal nucleus	+
Interanteromedial nucleus	±
Intermediodorsal nucleus	+
Lateral geniculate nucleus, dorsal*	+++
Lateral geniculate nucleus, ventral*†	+
Lateral habenular nucleus	±
Lateral posterior nucleus	+++
Laterodorsal nucleus	+++
Medial geniculate nucleus, dorsal	++
Medial geniculate nucleus, medial	++
Medial geniculate nucleus, ventral	++
Medial habenular nucleus	+
Mediodorsal nucleus	+
Nucleus reuniens	+++
Paracentral nucleus	++
Parafascicular nucleus*†	++++
Paratenial nucleus	++
Paraventricular nucleus, anterior	+
Posteromedian nucleus	+
Posterior nuclear group	++
Reticular nucleus	+++
Rhomboid nucleus	+
Subincertal nucleus*†	+
Submedius nucleus	++
Suprageniculate nucleus	+
Ventral anterior nucleus	+++
Ventral posterolateral nucleus	++++
Ventral posteromedial nucleus	++++
Ventrolateral nucleus	++++
Ventromedial nucleus*†	++++
Zona incerta*†	++
Hypothalamus	
Anterior hypothalamic area*†	+
Arcuate nucleus*	+
Lateral hypothalamic area*†	+
Lateral mammillary nucleus	++
Medial mammillary nucleus	++
Paraventricular nucleus, anterior parvicellular*	+
Paraventricular nucleus, lateral magnocellular*	+
Paraventricular nucleus, medial magnocellular*	+
Paraventricular nucleus, medial parvicellular	±
Paraventricular nucleus, posterior*†	+
Paraventricular nucleus, ventral*	+
Perifornical area*†	+
Posterior hypothalamic area*	+
Supraoptic nucleus	+
Ventromedial nucleus, central*	+
Ventromedial nucleus, dorsomedial*†	+
Ventromedial nucleus, ventrolateral*	+
Midbrain, pons and medulla oblongata	
Anterior tegmental nucleus*†	+
Anteroventral cochlear nucleus	+++

Table continues on following page

Table 1 (contd.)

Region	Expression
Area postrema*	+
Cuneate nucleus	+
Dorsal motor nucleus of the vagus*†	++
Dorsal raphe*	+
Dorsal tegmental nucleus	+
Facial nucleus	+++
Gigantocellular reticular nucleus*†	++
Hypoglossal nucleus*†	++
Inferior colliculus*†	++
Intermediate reticular nucleus*†	+
Interpeduncular nucleus*†	+
Lateral parabrachial nucleus, external lateral*†	+
Lateral parabrachial nucleus, internal lateral*	+
Laterodorsal tegmental nucleus*†	+
Locus ceruleus	+
Medial accessory oculomotor nucleus	+
Medial parabrachial nucleus	+
Median raphe*	+
Medullary reticular nucleus*	+
Mesencephalic tegmental nucleus	+++
Motor trigeminal nucleus	+++
Nucleus abducens	+
Nucleus ambiguus*†	+
Nucleus of the lateral lemnicsus	++
Nucleus of the solitary tract*†	+
Nucleus of the trapezoid body	++
Oculomotor nucleus	+
Olive	+
Paramedian raphe*	+
Parvicellular reticular nucleus*†	+
Pedunclopontine tegmental nucleus*†	+
Periaqueductal gray, ventrolateral*†	+
Pontine nuclei	++
Pontine reticular nucleus*†	++
Pretectal nucleus, anterior*†	+
Principal sensory trigeminal nucleus	+
Raphe magnus*†	+
Red nucleus, parvicellular	++
Red nucleus, magnocellular	++
Reticular tegmental nucleus	++
Spinal trigeminal nucleus*	+
Superior colliculus, intermediate gray layer*†	+
Superior colliculus, intermediate white layer*†	+
Superior colliculus, deep gray layer*†	+
Superior colliculus, deep white layer*†	+
Superior colliculus, optic layer*†	+++
Superior vestibular nucleus	+
Ventral cochlear nucleus, posterior	++
Ventral tegmental nucleus	+
Ventrolateral tegmental nucleus	+
Vestibular nucleus, lateral	+
Vestibular nucleus, medial*†	+

respectively [31]. Similarly, we found ALP-positive, MC4-R-positive cells in the perifornical part of the lateral hypothalamic area (Figures 7G and 7H), which contains neurons that innervate both autonomic preganglionic populations. Moreover, we observed ALP mRNA in most of the MC4-R-positive DMV cells (Figure 7J and 7K), which co-express choline acetyltransferase mRNA [17,23], indicating that they are parasympathetic preganglionic neurons. The DMV is one of the most dense sites of MC4-R expression in the entire CNS [16]. The co-expression of ALP and MC4-R transcripts in certain brain areas provides important evidence for their potential interaction *in vivo*.

The mouse ALP protein is the mouse orthologue of a human protein (KIAA0534), sharing 97 % similarity in the C-terminal part, and is 63 % similar to the C-terminal part of the mouse attractin protein (Figure 1). ALP and attractin proteins contain in their intracellular parts a highly conserved eight-amino-acid motif (MASRPFAS) whose function is unknown [20,29]. This motif seems not to participate in the interaction with the MC4-R. The amino acid sequence in the ALP C-terminus involved in the interaction with MC4-R could be dissected into two regions: one (residues 1280–1295) contains multiple changes in charge compared with the attractin sequence that might be responsible for the specificity of the interaction with MC4-R, and a second region (residues 1296–1316) sharing higher identity with attractin, with only one change in charge at position 1305. Also, a weak interaction was seen with the construct (− 1280) and could be related to the presence of an Arg residue (position 1275), because the substitution of this residue with Asn, as in the attractin sequence, produces a protein that does not bind the MC4-R C-terminal tail (results not shown).

Previous work has suggested that the mahogany/attractin protein may play a role in mediating the correct neuronal architecture necessary for delivery of agonist or antagonist to the site of the melanocortin receptor [32]. Moreover, *in vitro* studies demonstrate that attractin binds agouti protein, but not AGRP; furthermore, the absence of attractin does not suppress AGRP-induced obesity *in vivo* [21]. Therefore it is tempting to speculate on a possible functional role of ALP as a protein required for the action of AGRP. ALP may act as an AGRP co-receptor, modulating the AGRP–MC4-R interaction by altering the concentration, stability or conformation of AGRP at the MC4-R site, or, alternatively, by facilitating AGRP-induced MC4-R desensitization, uncoupling the receptor from the G-protein or stimulating internalization. Alternatively, ALP may play a role in the clustering and the synaptic localization of MC4-R.

The pattern of expression of ALP also suggests a function independent of this signalling pathway. ALP shows a similar, although not identical, pattern of expression to attractin, and these proteins may play overlapping and/or redundant roles. In spite of the role of attractin as an agouti co-receptor, other roles have been reported. Attractin could be involved in myelination and protection against oxidative stress in the CNS [19,33–35]. More recently, additional insight into the signalling pathway of attractin came from the identification and characterization of mouse Mahogunin (*Mgrn1*), the gene mutated in *mahoganoid* causing a similar phenotype to *mahogany*, as an E3 ubiquitin ligase that could be a candidate for mediating signalling through attractin [36]. There is one additional paralogue of Mahogunin (*Mgrn2*) in mouse and human that might be involved in ALP signalling. The study of attractin genetic models has focused on the CNS; to date, there is no report on the biochemical functions of attractin in peripheral tissue, except in T-lymphocytes in humans [30,37].

Although the pattern of ALP expression in the brain and periphery argues for a variety of functions for this protein, our findings of a direct interaction between the C-termini of mouse ALP and mouse MC4-R, the co-expression of these two transcripts in a variety of brain areas, and the pre-existing genetic data suggesting an interaction between attractin and the melanocortin 1 receptor provide us with reason to speculate that ALP is important in the MC4-R signalling pathway.

We thank Suzanne Deschesnes, Ruth Thomas and members of the Soderling, Stork and Goodman laboratories for their helpful suggestions and comments. This work was supported by grant DK51730 from the National Institutes of Health to R. D. C., by a National Research Service Award F32 to A. M. H., by fellowships from Fondation Bettencourt-Schueller and Fondation pour la Recherche Medicale to P. R., and by grants DK53301 and MH61583 to J. K. E.

REFERENCES

1 Fan, W., Boston, B. A., Kesterson, R. A., Hruby, V. J. and Cone, R. D. (1997) Role of melanocortinergic neurons in feeding and the agouti obesity syndrome. Nature (London) **385**, 165–168
2 Fan, W., Dinulescu, D. M., Butler, A. A., Zhou, J., Marks, D. L. and Cone, R. D. (2000) The central melanocortin system can directly regulate serum insulin levels. Endocrinology **141**, 3072–3079
3 Huszar, D., Lynch, C. A., Fairchild-Huntress, V., Dunmore, J. H., Fang, Q., Berkemeier, L. R., Gu, W., Kesterson, R. A., Boston, B. A., Cone, R. D. et al. (1997) Targeted disruption of the melanocortin-4 receptor results in obesity in mice. Cell **88**, 131–141
4 Graham, M., Shutter, J. R., Sarmiento, U., Sarosi, I. and Stark, K. L. (1997) Overexpression of Agrt leads to obesity in transgenic mice. Nat. Genet. **17**, 273–274
5 Yaswen, L., Diehl, N., Brennan, M. B. and Hochgeschwender, U. (1999) Obesity in the mouse model of pro-opiomelanocortin deficiency responds to peripheral melanocortin. Nat. Med. **5**, 1066–1070
6 Michaud, E. J., Bultman, S. J., Klebig, M. L., van Vugt, M. J., Stubbs, L. J., Russell, L. B. and Woychik, R. P. (1994) A molecular model for the genetic and phenotypic characteristics of the mouse lethal yellow (Ay) mutation. Proc. Natl. Acad. Sci. U.S.A. **91**, 2562–2566
7 Duhl, D. M., Stevens, M. E., Vrieling, H., Saxon, P. J., Miller, M. W., Epstein, C. J. and Barsh, G. S. (1994) Pleiotropic effects of the mouse lethal yellow (Ay) mutation explained by deletion of a maternally expressed gene and the simultaneous production of agouti fusion RNAs. Development **120**, 1695–1708
8 Ollmann, M. M., Wilson, B. D., Yang, Y. K., Kerns, J. A., Chen, Y., Gantz, I. and Barsh, G. S. (1997) Antagonism of central melanocortin receptors *in vitro* and *in vivo* by agouti-related protein. Science **278**, 135–138
9 Krude, H., Biebermann, H., Luck, W., Horn, R., Brabant, G. and Gruters, A. (1998) Severe early-onset obesity, adrenal insufficiency and red hair pigmentation caused by POMC mutations in humans. Nat. Genet. **19**, 155–157
10 Vaisse, C., Clement, K., Guy-Grand, B. and Froguel, P. (1998) A frameshift mutation in human MC4-R is associated with a dominant form of obesity. Nat. Genet. **20**, 113–114
11 Yeo, G. S., Farooqi, I. S., Aminian, S., Halsall, D. J., Stanhope, R. G. and O'Rahilly, S. (1998) A frameshift mutation in MC4-R associated with dominantly inherited human obesity. Nat. Genet. **20**, 111–112
12 Hinney, A., Schmidt, A., Nottebom, K., Heibult, O., Becker, I., Ziegler, A., Gerber, G., Sina, M., Gorg, T., Mayer, H. et al. (1999) Several mutations in the melanocortin-4 receptor gene including a nonsense and a frameshift mutation associated with dominantly inherited obesity in humans. J. Clin. Endocrinol. Metab. **84**, 1483–1486
13 Gu, W., Tu, Z., Kleyn, P. W., Kissebah, A., Duprat, L., Lee, J., Chin, W., Maruti, S., Deng, N., Fisher, S. L. et al. (1999) Identification and functional analysis of novel human melanocortin-4 receptor variants. Diabetes **48**, 635–639
14 Farooqi, I. S., Yeo, G. S., Keogh, J. M., Aminian, S., Jebb, S. A., Butler, G., Cheetham, T. and O'Rahilly, S. (2000) Dominant and recessive inheritance of morbid obesity associated with melanocortin 4 receptor deficiency. J. Clin. Invest. **106**, 271–279
15 Cone, R. D. (2000) Haploinsufficiency of the melanocortin-4 receptor: part of a thrifty genotype? J. Clin. Invest. **106**, 185–187
16 Mountjoy, K. G., Mortrud, M. T., Low, M. J., Simerly, R. B. and Cone, R. D. (1994) Localization of the melanocortin-4 receptor (MC4-R) in neuroendocrine and autonomic control circuits in the brain. Mol. Endocrinol. **8**, 1298–1308
17 Kishi, T., Aschkenasi, C. J., Lee, C. E., Mountjoy, K. G., Saper, C. B. and Elmquist, J. K. (2003) Expression of melanocortin 4 receptor mRNA in the central nervous system of the rat. J. Comp. Neurol. **457**, 213–235
18 Miller, K. A., Gunn, T. M., Carrasquillo, M. M., Lamoreux, M. L., Galbraith, D. B. and Barsh, G. S. (1997) Genetic studies of the mouse mutations mahogany and mahoganoid. Genetics **146**, 1407–1415
19 Gunn, T. M., Inui, T., Kitada, K., Ito, S., Wakamatsu, K., He, L., Bouley, D. M., Serikawa, T. and Barsh, G. S. (2001) Molecular and phenotypic analysis of Attractin mutant mice. Genetics **158**, 1683–1695
20 Nagle, D. L., McGrail, S. H., Vitale, J., Woolf, E. A., Dussault, Jr, B. J., DiRocco, L., Holmgren, L., Montagno, J., Bork, P., Huszar, D. et al. (1999) The mahogany protein is a receptor involved in suppression of obesity. Nature (London) **398**, 148–152
21 He, L., Gunn, T. M., Bouley, D. M., Lu, X. Y., Watson, S. J., Schlossman, S. F., Duke-Cohan, J. S. and Barsh, G. S. (2001) A biochemical function for attractin in agouti-induced pigmentation and obesity. Nat. Genet. **27**, 40–47
22 Lu, X., Gunn, T. M., Shieh, K., Barsh, G. S., Akil, H. and Watson, S. J. (1999) Distribution of Mahogany/Attractin mRNA in the rat central nervous system. FEBS Lett. **462**, 101–107
23 Liu, H., Kishi, T., Roseberry, A. G., Cai, X., Lee, C. E., Montez, J. M., Friedman, J. M. and Elmquist, J. K. (2003) Transgenic mice expressing green fluorescent protein under the control of the melanocortin-4 receptor promoter. J. Neurosci. **23**, 7143–7154
24 Simmons, D. M., Arriza, J. L. and Swanson, L. W. (1989) A complete protocol for *in situ* hybridization of messenger RNAs in brain and other tissues with radiolabelled single stranded RNA probes. J. Histotechnol. **12**, 169–181
25 Marcus, J. N., Aschkenasi, C. J., Lee, C. E., Chemelli, R. M., Saper, C. B., Yanagisawa, M. and Elmquist, J. K. (2001) Differential expression of orexin receptors 1 and 2 in the rat brain. J. Comp. Neurol. **435**, 6–25
26 Elias, C. F., Saper, C. B., Maratos-Flier, E., Tritos, N. A., Lee, C., Kelly, J., Tatro, J. B., Hoffman, G. E., Ollmann, M. M., Barsh, G. S. et al. (1998) Chemically defined projections linking the mediobasal hypothalamus and the lateral hypothalamic area. J. Comp. Neurol. **402**, 442–459
27 Elias, C. F., Aschkenasi, C., Lee, C., Kelly, J., Ahima, R. S., Bjorbaek, C., Flier, J. S., Saper, C. B. and Elmquist, J. K. (1999) Leptin differentially regulates NPY and POMC neurons projecting to the lateral hypothalamic area. Neuron **23**, 775–786
27a Franklin, K. B. J. and Paxions, G. (2001) The Mouse Brain in Sterotaxic Coordinates, 2nd edn, Academic Press, San Diego
28 Shinyama, H., Masuzaki, H., Fang, H. and Flier, J. S. (2003) Regulation of melanocortin-4 receptor signaling: agonist-mediated desensitization and internalization. Endocrinology **144**, 1301–1314
29 Gunn, T. M., Miller, K. A., He, L., Hyman, R. W., Davis, R. W., Azarani, A., Schlossman, S. F., Duke-Cohan, J. S. and Barsh, G. S. (1999) The mouse mahogany locus encodes a transmembrane form of human attractin. Nature (London) **398**, 152–156
30 Tang, W., Gunn, T. M., McLaughlin, D. F., Barsh, G. S., Schlossman, S. F. and Duke-Cohan, J. S. (2000) Secreted and membrane attractin result from alternative splicing of the human ATRN gene. Proc. Natl. Acad. Sci. U.S.A. **97**, 6025–6030
31 Saper, C. B. (1995) The spinoparabrachial pathway: shedding new light on an old path. J. Comp. Neurol. **353**, 477–479
32 Dinulescu, D. M. and Cone, R. D. (2000) Agouti and agouti-related protein: analogies and contrasts. J. Biol. Chem. **275**, 6695–6698
33 Kuramoto, T., Kitada, K., Inui, T., Sasaki, Y., Ito, K., Hase, T., Kawagachi, S., Ogawa, Y., Nakao, K., Barsh, G. S. et al. (2001) Attractin/mahogany/zitter plays a critical role in myelination of the central nervous system. Proc. Natl. Acad. Sci. U.S.A. **98**, 559–564
34 Kuwamura, M., Maeda, M., Kuramoto, T., Kitada, K., Kanehara, T., Moriyama, M., Nakane, Y., Yamate, J., Ushijima, T., Kotani, T. and Serikawa, T. (2002) The myelin vacuolation (mv) rat with a null mutation in the attractin gene. Lab. Invest. **82**, 1279–1286
35 Muto, Y. and Sato, K. (2003) Pivotal role of attractin in cell survival under oxidative stress in the zitter rat brain with genetic spongiform encephalopathy. Brain Res. Mol. Brain Res. **111**, 111–122
36 He, L., Eldridge, A. G., Jackson, P. K., Gunn, T. M. and Barsh, G. S. (2003) Accessory proteins for melanocortin signaling: attractin and mahogunin. Ann. N.Y. Acad. Sci. **994**, 288–298
37 Duke-Cohan, J. S., Gu, J., McLaughlin, D. F., Xu, Y., Freeman, G. J. and Schlossman, S. F. (1998) Attractin (DPPT-L), a member of the CUB family of cell adhesion and guidance proteins, is secreted by activated human T lymphocytes and modulates immune cell interactions. Proc. Natl. Acad. Sci. U.S.A. **95**, 11336–11341

Received 14 August 2003/15 September 2003; accepted 7 October 2003
Published as BJ Immediate Publication 7 October 2003, DOI 10.1042/BJ20031241